

Process Control for Additive Manufacturing of Concrete Components

Lukas Lachmayer¹[0000-0001-8070-8989], Robin Dörrie²[0000-0001-8473-7218],
Harald Kloft²[0000-0003-4891-869X] and Annika Raatz¹[0000-0002-1697-1907]

¹ Institute of Assembly Technology, Leibniz University Hannover, Germany

² Institute for Structural Design, Technische Universität Braunschweig, Germany
lachmayer@match.uni-hannover.de

Abstract. Additive manufacturing (AM) processes offer new possibilities in the design of concrete components. The process chain for AM processes generally consists of component design, print path generation, and manufacturing. Within the step of print path generation, the component is commonly divided into layers and filled with waypoints based on the assumption of a constant cross-section of the applied material strands. In contrast to metal or plastic, however, the material properties of fresh concrete are more sensitive to environmental influences such as temperature and humidity. This leads to cross-section variations during the process. Therefore, exclusively relying on an a priori print path planning for large-scale components leads to significant deviations between as-planned and as-printed geometries. The presented research aims to increase the manufacturing accuracy of concrete components by compensating layer inconsistencies through a controlled material application. For this purpose, varying the printing speed and nozzle distance allows for correction of the deviations of subjacent layers. Deviation detection is performed by a 2D laser sensor mounted on the printing nozzle to generate information about the underlying cross-section. Comparing the measured values to precalculated setpoints generates the error values. The control algorithm maps the error data into an adaption of the printing speed and nozzle distance to fulfill the pre-planned geometry. Applying the controller to a medium-sized component and comparing the result to the uncontrolled process shows a considerable accuracy improvement.

Keywords: Shotcrete 3D printing, Process Control, Additive Manufacturing.

1 Introduction

In relation to commercial 3D printing applications, additive manufacturing processes open new design possibilities for the construction industry. Thereby, complex designs, such as topologically optimized components, function integration, and sustainable wastage reduction, are within the scope of affiliated research for structural concrete components [1]. The ITE TU Braunschweig proposes a highly flexible Shotcrete 3D Printing (SC3DP) process to achieve the preset goals without the use of formwork. In

contrast to extrusion processes, fresh concrete is mixed with pressurized air at the printing nozzle and applied by jetting as shown in Fig. 1 a) [2]. However, concrete printing processes offer new challenges for ensuring sufficient component quality. On the one hand, the flowability of fresh concrete will cause material deformation throughout the printing [3]. On the other hand, the material properties are significantly affected by the environmental conditions. Therefore, heating of the production system leads to varying concrete strand geometries during the production process [4]. In addition, the introduced SC3DP is initially unstable. Due to the spray cone, production errors regarding the targeted layer height \hat{h}_L lead to a constantly in- or decreasing actual nozzle distance d_N . As shown in Fig. 1 b), a negative error e_1 during production induce an enhanced spray distance, which consequently produces a wider but lower strand. Since the position of the nozzle is not adapted in the second layer n_2 , the error e_2 increases in the following layer.

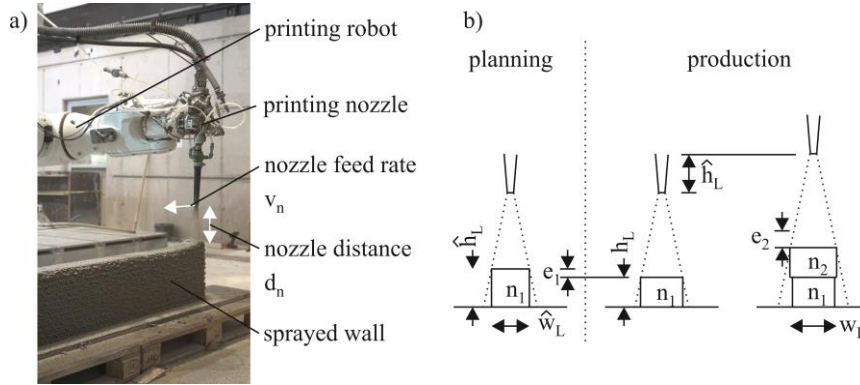


Fig. 1. a) Shotcrete 3D printing process at DBFL ITE TU Braunschweig b) Unstable printing behavior due to production error in the first layer

Within this paper, we present a control algorithm to stabilize the process and enable the production of more accurate components. The algorithm utilizes a 2D laser scanner mounted on the printing nozzle to recognize the width w_L of the previously printed layers to adjust the nozzle distance d_N . Thereby, we achieve the as-planned layer width \hat{w}_L . Furthermore, the algorithm measures the distance between the printing nozzle and the previously printed layer to adjust the printing feed rate v_N . This compensates for deviations in the produced layer height h_L .

2 Related Work

Initial approaches to stabilize the 3D concrete printing process are given by Grim-scheid et al. [5]. The authors use cross-section evaluation to set specific process parameters to achieve the desired layer geometry for shotcrete tunnel reinforcement. However, no feedback is implemented and, thus, deviations about 2 cm per layer must be

expected. A more complex control strategy including a feedback loop was proposed by Wolfs et al. [6]. The authors use a 1D Time-of-Flight distance measurement system to evaluate the clearance between the printing nozzle and the previously fabricated layer. An error is calculated by comparing the measured distance with the targeted values. This value is used to correct the z-coordinate of the printing system, leading to less deformed layers and higher end component quality. However, it must be said that the final component height will not match the designed geometries due to correction of the nozzle position. A similar control approach is presented by Ibrahim et al. [7]. The authors also detect the distance between the printing nozzle and the applied layer. However, they used the printing speed to correct the amount of applied material and thereby adjust the layer height. In relation to the previous algorithm [6] this will ensure the final component height. While the current state of research clearly outlines the necessity of controlled concrete printing, the previous one does not consider the strand width. In addition to the lack of width control, there is only little research on controller parameterization, controller design, and comparison to uncontrolled printing.

3 Experimental Setup

For experimental investigations, we utilize the shotcrete 3D printing process at the digital building fabrication laboratory (DBFL) at the ITE, which is part of the TU Braunschweig. The printing system consists of a 6-DoF TX 200 Stäubli attached to a 3-DoF portal structure. For material supply, batches of 75 kg of reinforced plain cement concrete, produced by MC Bauchemie Müller, are mixed with a WM-Jetmix 125 Mixer by Werner Mader GmbH. A WM-Variojet FU Pump pumps the material through 25 m hoses to the printing nozzle, where pressurized air generates a material spraying process. For real-time recognition of the geometrical properties of the printed strands, the robot is equipped with a 2D laser scanner, as shown in Fig. 2.

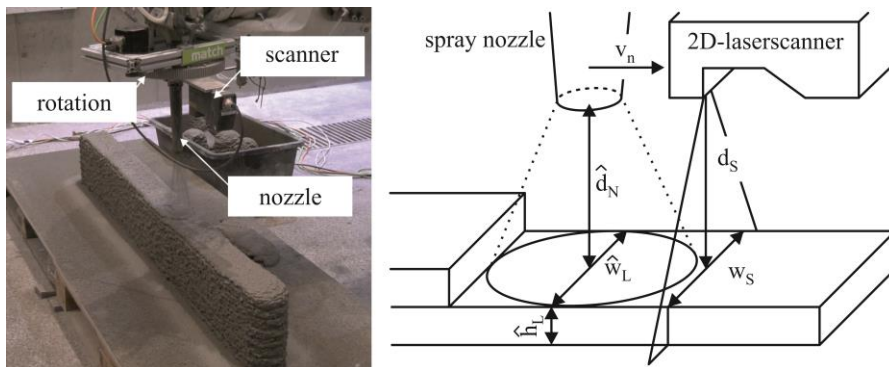


Fig. 2. SC3DP at DBFL TU Braunschweig with added scanning system for real-time cross-section control by comparing w_S and d_S with the target values \hat{w}_L and \hat{d}_N .

The scanner runs ahead of the printing process, recognizing the layer width w_S and the distance d_S between the scanner and the applied material.

4 Algorithm

For the design of our control algorithm, we assume that our production system's positioning accuracy is higher than the required component precision. This is the case for most stationary production systems and allows utilization of the printing nozzle as a reference point. Given the reference and a predefined printing path planned with defined nozzle distances \hat{d}_N , these distances must be controlled and adhered to ensure final component height in the subsequent printing process. The controller itself is based on the following principle: a reduction of the measured nozzle distance d_S will indicate too much material, while an increase indicates too little material, in the previous layer.

To compensate for such distance deviations, our algorithm varies the nozzle feed rate v_N to apply either more or less material. Besides maintaining the desired nozzle distance \hat{d}_N , the layer width w_L is controlled. While the feed rate significantly influences the layer height, the width is strongly affected by the spray distance. Therefore, the algorithm utilizes spray distance variation to achieve the planned layer width \hat{w}_L .

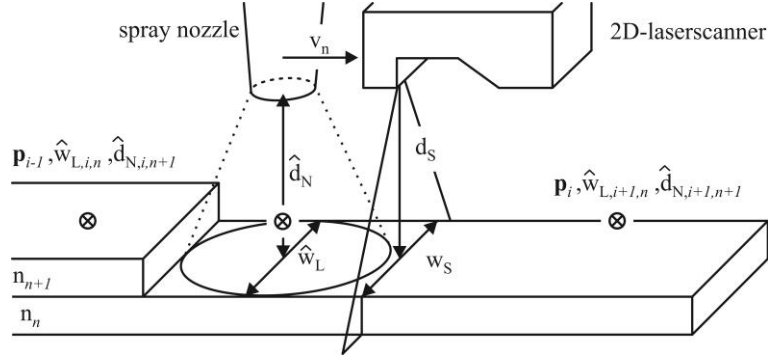


Fig. 3. Required variables at each path point for full control of the layer width and height during shotcrete 3D printing experiments.

For a continuous deviation correction, the control algorithm constantly requires target values for \hat{w}_L and \hat{d}_N . Therefore, we provided $\hat{w}_{L,i,n}$ and $\hat{d}_{N,i,n+1}$ for each path point \mathbf{p}_{i-1} as shown in Fig. 3. Since the provided target width and distance belong to the next point \mathbf{p}_i , we can linearly interpolate the distance values for the upcoming movement by equation (1) and use the actual robot position \mathbf{p} for evaluation.

$$\frac{(\hat{d}_{N,i+1,n+1} - \hat{d}_{N,i,n+1})}{\|\mathbf{p}_i - \mathbf{p}_{i-1}\|_2} * \|\mathbf{p} - \mathbf{p}_{i-1}\|_2 + \hat{d}_{N,0} = \hat{d}_N \quad (1)$$

A similar linear interpolation is used to calculate \hat{w}_L . Due to the laser scanner positioning, we track the layer width of the previous layer n_n and thus, $\hat{w}_{L,i,n}$ and $\hat{w}_{L,i+1,n}$ are used. The inclination and the y-intercept of the interpolation are recalculated whenever the robot reaches a new path point. Since the scanner is running ahead of the printing nozzle, the actual measured values for w_S and d_S do not correlate with the target values \hat{w}_L and \hat{d}_N . To overcome this, the algorithm initially stores the measured values. Whenever the production system has moved for the distance between the nozzle and the scanner, the actual target values are compared with the previously recorded data from the list. The error values are calculated by equation (2) and (3).

$$\hat{d}_N - d_S = \Delta d \quad (2)$$

$$\hat{w}_N - w_S = \Delta w \quad (3)$$

For compensation of width deviations, the algorithm sums up all Δw errors within one layer and divides them by the number of measurements. When transferring from the actual printed layer n_n to n_{n+1} , the average width error is multiplied with $K_{p,w}$, empirically tuned to 0.5. The resulting value is added as an offset to the z-coordinates of the printing path. This offset affects the spray distance and thereby the scanner position and, therefore must be added to the target values of the nozzle distance. To feed back the nozzle distance error, another P-controller is implemented. The gain factor $K_{p,d}$ is set to 100. Additional robustness is added by averaging 10 measured values and ignoring deviations below 10 mm and above 60 mm.

5 Evaluation and Outlook

We evaluated the proposed algorithm by printing a 450·120·1600 mm wall segment with and without process control. As shown in Fig. 4 a), the proposed algorithm incrementally adjusts the nozzle distance to achieve the target layer width of 120 mm.

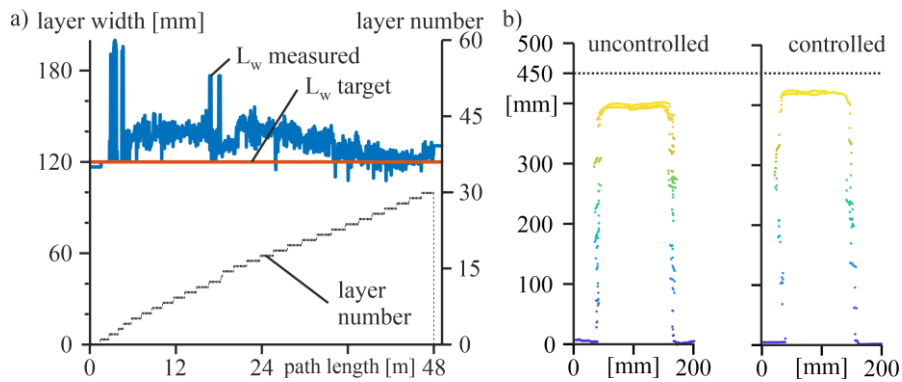


Fig. 4. a) Evaluation of the layer width development over the production process b) Comparison of uncontrolled and controlled component regarding the overall component height.

Due to mechanical issues, the process was restarted at the 15th layer, resulting in a step within the recorded width data and a reset of the converging control algorithm. Fig. 4 b) compares the overall height of the uncontrolled and controlled component based on sliced 3D point clouds recorded during the process. Considering the height tolerance of $\pm 10 \text{ mm}$, the final controlled component height deviation is 22 mm and thus improved by 26 mm according to the uncontrolled process.

The proposed algorithm can increase the overall height accuracy and shows convergence in terms of the layer width adjustment. While it stabilizes the printing process, it cannot prevent elastic buckling or plastic collapse and thereby component loss due to material failure. Therefore, we will investigate the possibility of integrating previously developed FEM methods [8] into the path planning algorithms to ensure component stability.

6 Acknowledgements

The authors gratefully acknowledge the funding by the Deutsche Forschungsgemeinschaft (DFG – German Research Foundation) – Project no. 414265976. The authors would like to thank the DFG for the support within the SFB/Transregio 277 – Additive manufacturing in construction. (Subproject B04 and A04)

References

1. Lowke, D., Dini, E., Perrot, A., Weger, D., Gehlen, C., Dillenburger, B.: Particle-bed 3D printing in concrete construction – Possibilities and challenges. *Cement and Concrete Research* 112, 50-65 (2018)
2. Lindemann, H., Gerbers, R., Ibrahim, S., Dietrich, F., Herrmann, E., Dröder, K., Raatz, A., Kloft, H.: Development of a Shotcrete 3D-Printing (SC3DP) Technology for Additive Manufacturing of Reinforced Freeform Concrete Structures. In: *First RILEM International Conference on Concrete and Digital Fabrication*, Springer, pp. 287-298 (2018)
3. Suiker, A. S. J., Wolfs, R. J. M., Lucs, S. M., Salet, T. A. M.: Elastic buckling and plastic collapse during 3D printing. *Cement and Concrete Research* 135, 1-17 (2020)
4. Niu, D., Zhang, S., Wang, Y., Hong, M., Li, Z.: Effect of temperature on strength, hydration products and microstructure of shotcrete blended with supplementary cementitious materials. *Construction and Building Materials* 264, 1-16 (2020)
5. Grimscheid, G., Moser, S.: Fully Automated Shotcrete Robot for Rock Support. *Computer-Aided Civil and Infrastructure Engineering* 16, 200-2015 (2001)
6. Wolfs, R. J. M., Bos, F. P., Strien, C. F., Salet, T. A. M.: A Real-Time Height Measurement and Feedback System for 3D Concrete Printing. In: *High Tech Concrete: Where Technology and Engineering Meet*, Springer, pp. 2474-2483 (2017)
7. Ibrahim, S., Olbrich, A., Lindemann, H., Gerbers, R., Klorf, H., Dröder, K., Raatz, A.: Automated Additive Manufacturing of Concrete Structures without Formwork – Concept for Path Planning. In: *Tagungsband des 3 Kongresses Montage Handhabung Industrieroboter*, Springer, pp. 83-91 (2018)
8. Lachmayer, L., Ekanayaka, V., Hürkamp, A., Raatz, A.: Approach to an optimized printing path for additive manufacturing in construction utilizing FEM modelling. In: *Procedia CIRP* 104, pp. 600-605 (2021)